

# Synthesis of Amphiphilic Poly(organosiloxane) Nanospheres with Different Core–Shell Architectures

Nadja Jungmann, Manfred Schmidt, and Michael Maskos\*

*Institut für Physikalische Chemie, Universität Mainz, Welter-Weg 11, D-55099 Mainz, Germany*

Johann Weis and Jochen Ebenhoch

*Wacker-Chemie GmbH, D-84480 Burghausen, Germany*

*Received December 10, 2001; Revised Manuscript Received June 24, 2002*

**ABSTRACT:** Core–shell and core–shell–shell nanospheres with different amphiphilicities were synthesized by sequential condensation of trimethoxymethylsilane (T), diethoxydimethylsilane (D), and the functional monomer (chloromethylphenyl)trimethoxysilane (ClBz-T) and mixtures thereof. The condensation was performed in aqueous dispersion in the presence of surfactant. Saturation of reactive surface SiOH groups with monofunctional trimethylsilane monomers prevents interparticle condensation and leads to nanoparticles, which are redispersable in organic solvents. The diameters of the particles range between 20 and 40 nm, depending on the composition. The thickness of the outer, nonfunctionalized shell is determined by asymmetrical flow field–flow fractionation (AF–FFF) and dynamic light scattering (DLS) of the core and core–shell particles, respectively. It varies between 1.5 and 3 nm and is proportional to the volume of added monomer. Incorporating (chloromethylphenyl)siloxane groups in the core and performing a subsequent quaternization reaction of dimethylaminoethanol yield amphiphilic nanospheres with an ionic, hydrophilic core and a hydrophobic outer shell. The amount of ionic moieties is found to be proportional to the amount of functional (chloromethylphenyl)siloxane groups incorporated in the spheres. Additionally, multiple shell topologies were successfully prepared, i.e., particles with a poly(dimethylsiloxane) (PDMS) core, an ionic inner and a hydrophobic outer shell. If linear PDMS chains forming the core are prevented to chemically bind to the inner shell, they may be removed by ultrafiltration, resulting in the formation of hollow spheres.

## Introduction

Amphiphilic core–shell nanoparticles are of steadily growing interest. Existing systems include nanoparticles based on the self-assembly of amphiphilic block copolymers and subsequent selective cross-linking<sup>1–3</sup> and polyelectrolyte capsules,<sup>4</sup> to quote only a few representative species. So far, the first systems mentioned yield core–shell nanoparticles with one or two shells, depending on the block copolymer employed. A template is used in the second system to adsorb alternating layers of different polyelectrolytes and a shell is formed. Hollow capsules are obtained, if the template is removed. We would like to present an approach that combines the individual advantages of the several different systems in one synthetic procedure and allows one to control (i) the size of the particles, (ii) the thickness and number of shells, (iii) the amphiphilic properties, (iv) the network density, and (v) the spherical architecture, including hollow amphiphilic nanoparticles.

In this paper, we utilize a chemical system based on poly(organosiloxane)s. First, the organosilane monomers are condensed via the sol–gel process in aqueous dispersion.<sup>5–9</sup> Sequential addition of the monomers leads to the formation of spherical core–shell colloids with diameters of 5 nm up to about 100 nm. The particles are then transferred into an organic solvent and, after saturation of the reactive surface groups, can be isolated and are redispersable. Finally, a polymer analogous reaction is performed to obtain amphiphilic poly(organosiloxane) nanoparticles. Figure 1 contains a schematic description of the synthesis.

At the beginning of the synthesis, mixtures of trimethoxymethylsilane (T), (chloromethylphenyl)trimeth-

oxysilane (ClBz-T), and diethoxydimethylsilane (D) are added sequentially and co-condense in the presence of the surfactant benzethonium chloride. The monomers T and D form the hydrophobic parts of the colloids, while ClBz-T is later on transformed into electrolyte moieties, leading to the formation of hydrophilic domains. Furthermore, the ratio of T and D controls the network density of the nanospheres, because the T units act as cross linker, while the D units form chain elements. The resulting nanonetworks are less dense and show a higher elasticity as compared to silica particles based on tetraethoxysilane (TEOS).<sup>9,10</sup> The resulting nanoparticles are also smaller due to the stabilizing effect of the surfactant.

The versatile synthesis allows the formation of multiple shell topologies with varying content of ClBz-T groups and thus, after quaternization, the building of amphiphilic nanospheres with varying hydrophilic properties. The amphiphilic nanoparticles may be used to transfer small hydrophilic molecules into the organic phase. For potential applications it is therefore of major importance that the network is penetrable for small molecules, which can be adjusted, as already mentioned.

## Experimental Section

**Materials.** Water was purified with a milliQ deionizing system (Waters, Germany). Trimethoxymethylsilane (T), diethoxydimethylsilane (D), ethoxytrimethylsilane (M), hexamethyldisilazane (HMN) (Wacker Chemie), tetrahydrofuran (Riedel deHäen), toluene, methanol, cyclohexane (Merck), sodium hydroxide, dimethylaminoethanol, TWEEN 20 (Fluka), benzethonium chloride ([2[2-(*p*-1,1–3,3-tetramethylbutylphenoxy)ethoxy]ethyl]ammonium chloride, Aldrich), and (*p*-chloromethylphenyl)trimethoxysilane (ClBz-T) (ABCR, Germany) were used as received.

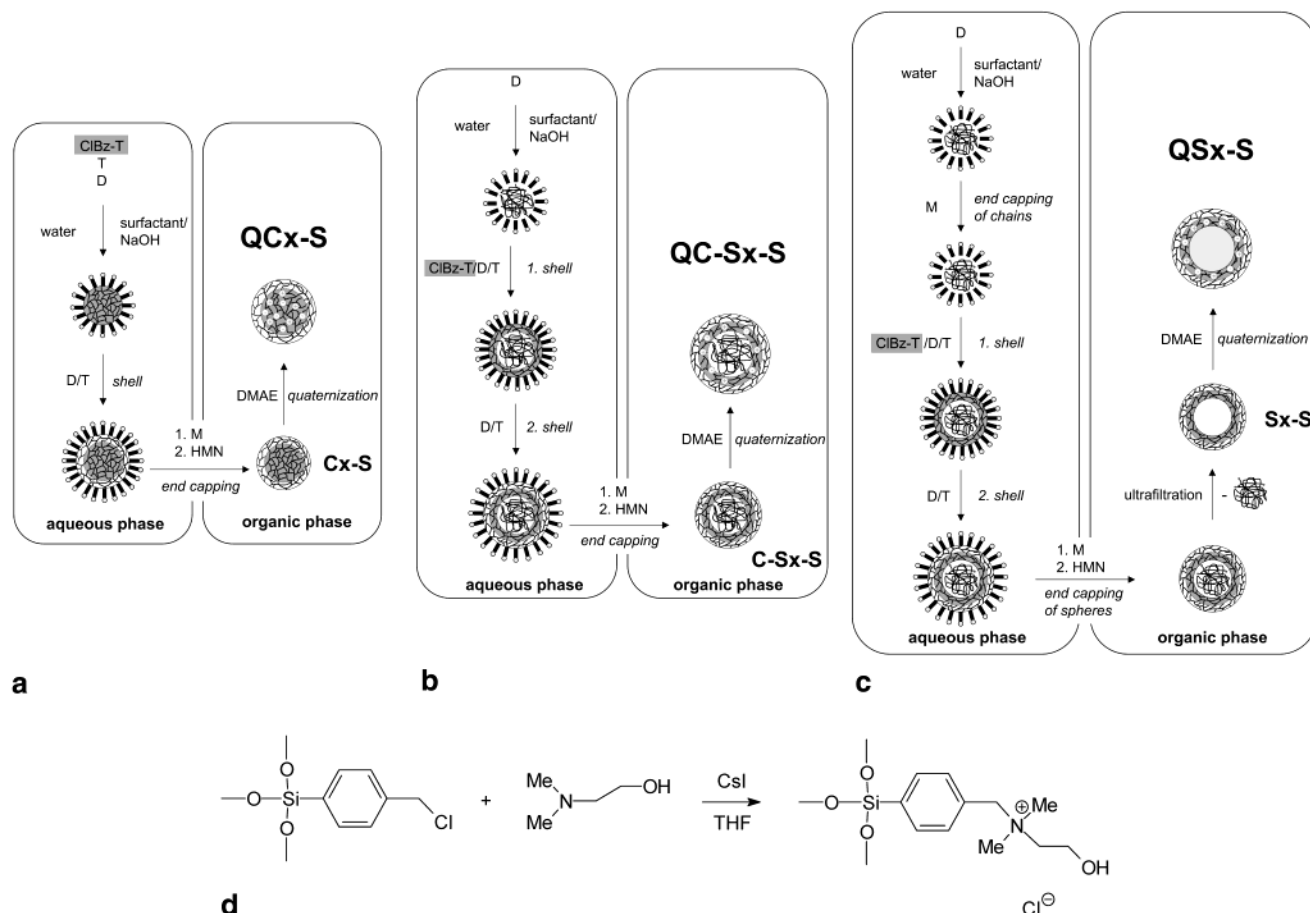


**Figure 1.** Reaction schemes for the synthesis of nanospheres with functionalized core, QCx-S (a), poly(dimethylsiloxane) (PDMS) core and functionalized inner shell, QC-Sx-S (b), and hollow nanoparticles with functionalized inner shell, QSx-S (c), respectively. T = trimethoxymethylsilane, D = diethoxydimethylsilane, CIBz-T = (chloromethylphenyl)trimethoxysilane, M = ethoxytrimethylsilane, HMN = hexamethyldisilazane,  $x$  = amount of CIBz-T employed in the synthesis. (d) Schematic representation of the quaternization reaction of dimethylaminoethanol (DMAE) leading to the formation of amphiphilic nanospheres.

**Instrumentation.** Dynamic light scattering (DLS) was performed with an argon ion laser (Stabilite 2060-04,  $\lambda = 514$  nm, Spectra-Physics), a SP-125 goniometer, and an ALV-5000 multiple-tau digital correlator at angles between 50 and 130° in steps of 20°. The temperature was kept constant at 293 K. The aqueous samples were filtered through Millex-GS filters (0.22  $\mu\text{m}$ ) and the organic solutions through Millex-FG (0.2  $\mu\text{m}$ ), Dimex-25 (0.2  $\mu\text{m}$ ), or Millex-SR filters (0.5  $\mu\text{m}$ , Millipore). The DLS data were analyzed by a cumulant fit and by a biexponential fit utilizing the simplex algorithm, respectively, to yield the angular dependent diffusion coefficient  $D_0$ . The extrapolation to zero scattering angle gives the diffusion coefficient  $D$  which is translated into the appropriate hydrodynamic radius via the Stokes–Einstein relation.<sup>11</sup>

Gel permeation chromatography (GPC) was performed in degassed toluene utilizing a Rheos 400 HPLC-pump (ERC) operating at 1 mL/min, Styragel columns (pore size 10<sup>5</sup>, 10<sup>4</sup>, 10<sup>3</sup>, PSS), and a Waters 410 refractive index detector.

The asymmetrical flow field–flow fractionation (AF–FFF) from Consensus consisted of an AF–FFF channel system 2.0. A Waters 486-UV detector operating at 254 nm monitored the eluting particles. Regenerated cellulose membranes were utilized as semipermeable walls (MWCO 10 000 g/mol). Degassed milliQ water with NaN<sub>3</sub> (200 mg/L) and the surfactant TWEEN 20 (100 mg/L) was used as eluent ( $\eta = 0.94$  cP).<sup>12</sup>

UV spectra in cyclohexane were recorded with a Lambda 17 UV spectrometer (Perkin-Elmer) and the FT-IR measurements with a Nicolet 55X spectrometer. The samples were dissolved in dichloromethane, deposited on NaCl plates, and analyzed after evaporation of the solvent.

The <sup>1</sup>H NMR spectra were recorded on a Bruker AM-400 spectrometer; the chemical shifts are obtained by comparison to the solvent CDCl<sub>3</sub>.

AFM measurements were performed with a Nanoscope IIIa scanning probe microscope (Digital Instruments) in tapping mode. The samples were spin cast from toluene ( $c = 0.1$  g/L) onto freshly cleaved mica.

**Synthesis.** Figure 1 shows the reaction scheme of the three different particle topologies. The  $x$  in the sample code refers to the amount of (chloromethylphenyl)trimethoxysilane monomer (CIBz-T) in the reaction mixture for the corresponding part of the particles ( $W_{\text{CIBz-T}}/W_{\text{total monomer}}$ ). The amount of the various monomers employed for each sample is given in Table 1.

**Core–Shell Spheres (Cx-S).** To a solution of 125 g of water, 300 mg of 10% (w/w) sodium hydroxide (0.75 mmol), and 2.5 g of benzethonium chloride (5.58 mmol,  $S = 0.10$ ;  $S$  = fleet ratio, defined as quotient of total mass of surfactant over total mass of nonhydrolyzed monomer) were added the pre-mixed monomers dropwise through a syringe pump (15 mL/h) under continuous mechanical stirring at room temperature. The solution was stirred for 1 week in order to ensure complete conversion, before the monomer mixture for the shell was added dropwise (10 mL/min) and the solution was stirred overnight.

**End Capping of Free SiOH Groups.** During the course of the reaction, a small amount of the material became stuck to the stirrer, and the dispersion was filtered before the end capping was performed. Subsequently, an aliquot containing 25 g of the dispersion was taken (the residual dispersion was stored for further investigations), 5 g (0.048 mol) of ethoxytrimethylsilane (M) was added, and the reaction was stirred overnight. An additional 2.5 g (0.024 mol) of M was added and stirred for 5 h. This dispersion was destabilized by addition of 100 mL of methanol and centrifuged. The precipitate was washed with 50 mL of methanol and centrifuged again. This step was repeated 2 times, and afterward the moist precipitate

**Table 1. Amount of Monomer D, T, and ClBz-T Used in Each Step of the Synthesis**

sample		D/(m/g)	T/(m/g)	ClBz-T/(m/g)	T <sub>total</sub> /% (w/w)
C4-S	core	5.0	9.0	1.0	66.7
	shell	3.0	7.0		70.0
	Σ	8.0	16.0	1.0	68.0
C8-S	core	5.0	8.0	2.0	66.7
	shell	3.0	7.0		70.0
	Σ	8.0	15.0	2.0	68.0
C12-S	core	5.0	7.0	3.0	66.7
	shell	3.0	7.0		70.0
	Σ	8.0	14.0	3.0	68.0
C-S4-S	core	8.0			
	1st shell	2.0	4.0	1.0	71.5
	2nd shell	3.0	7.0		70.0
	Σ	13.0	11.0	1.0	48.0
C-S8-S	core	8.0			
	1st shell	2.0	3.0	2.0	71.5
	2nd shell	3.0	7.0		70.0
	Σ	13.0	10.0	2.0	48.0
C-S12-S	core	8.0			
	1st shell	2.0	2.0	3.0	71.5
	2nd shell	3.0	7.0		70.0
	Σ	13.0	9.0	3.0	48.0
S4-S	core	8.0			
	1st shell	2.0	4.0	1.0	71.5
	2nd shell	3.0	7.0		70.0
	Σ	5.0	11.0	1.0	70.6
S8-S	core	8.0			
	1st shell	2.0	3.0	2.0	71.5
	2nd shell	3.0	7.0		70.0
	Σ	5.0	10.0	2.0	70.6
S12-S	core	8.0			
	1st shell	2.0	2.0	3.0	71.5
	2nd shell	3.0	7.0		70.0
	Σ	5.0	9.0	3.0	70.6

<sup>a</sup> The total amount of monomer is kept constant at 25 g. PDMS-core in Sx-S samples is removed by ultrafiltration and neglected in the calculation of T<sub>total</sub>.

was dissolved in 50 mL of toluene. Methanol and water were removed by means of rotary evaporation at 40 °C in a vacuum. To the remaining solution was added 1.6 g (9.94 mmol) of hexamethyldisilazane (HMN), and it was stirred overnight. The solution was precipitated into 150 mL of methanol, and the precipitate was collected by filtration. The resulting powder was lyophilized from benzene.

After end capping, this yielded 1.5–2.0 g of white powder (sample code Cx-S; x indicates the amount of ClBz-T monomer [w/w]).

IR,  $\tilde{\nu}/\text{cm}^{-1}$ : 2964, 2908 (s)  $\nu(\text{CH}_3)$ ,  $\nu(\text{CH}_2)$ , 1610 (m)  $\nu$ -(aromatic ring), 1396 (s)  $\delta(\text{CH}_3)$ ,  $\delta(\text{CH}_2)$ , 1270 (vs)  $\delta_s(\text{SiCH}_3)$ , 1131, 1030 (vs)  $\delta_{\text{as}}(\text{Si}-\text{O}-\text{Si})$ , 844, 796 (s)  $\delta(\text{SiCH}_3)$ .

<sup>1</sup>H NMR,  $\delta/\text{ppm}$ : 0–1.5 (s, br,  $\text{SiCH}_3$ ), 4.4 (m, br,  $\text{CH}_2\text{Cl}$ ), 7.0–7.6 (s, br, aromatic H).

**Core–Shell–Shell Spheres with PDMS Core Attached to the Surrounding Shell (C-Sx-S).** To a solution of 125 g of water, 600 mg of 10% (w/w) sodium hydroxide (1.50 mmol), and 2.0 g of benzethonium chloride (4.46 mmol, S = 0.08) was added 8 g (54 mmol) of diethoxydimethylsilane (D) dropwise through a syringe pump over 1 h under continuous mechanical stirring at room temperature. The dispersion was stirred overnight, and subsequently, the monomer mixture for the first shell was added according to Table 1 over a period of 1 h. After 1 week of stirring, the monomer mixture for the second shell was added dropwise within 1 h, and the dispersion was stirred overnight.

After end capping, this yielded 1.4–1.8 g of white powder (sample code C-Sx-S; x indicates the amount of ClBz-T monomer [w/w]).

IR,  $\tilde{\nu}/\text{cm}^{-1}$ : 2963, 2906 (s)  $\nu(\text{CH}_3)$ ,  $\nu(\text{CH}_2)$ , 1606 (m)  $\nu$ -(aromatic ring), 1410 (s)  $\delta(\text{CH}_3)$ ,  $\delta(\text{CH}_2)$ , 1260 (vs)  $\delta_s(\text{SiCH}_3)$ , 1129, 1030 (vs)  $\delta_{\text{as}}(\text{Si}-\text{O}-\text{Si})$ , 856, 803 (s)  $\delta(\text{SiCH}_3)$ .

<sup>1</sup>H NMR,  $\delta/\text{ppm}$ : 0–2.0 (s, br,  $\text{SiCH}_3$ ), 4.5 (m, br,  $\text{CH}_2\text{Cl}$ ), 7.0–7.8 (s, br, aromatic H).

**Core–Shell–Shell Spheres with PDMS-Core Not Attached to the Surrounding Shell (Sx-S).** To a solution of

125 g of water, 600 mg of 10% (w/w) sodium hydroxide (1.50 mmol), and 2.0 g of benzethonium chloride (4.46 mmol, S = 0.08) was added 8 g (54 mmol) of diethoxydimethylsilane (D) for the core dropwise through a syringe pump over 1 h under continuous mechanical stirring at room temperature. The dispersion was stirred overnight, and subsequently, 100 mg (0.96 mmol) of M was added. After 8 h, another 100 mg (0.96 mmol) of M was added, and the dispersion was stirred overnight. The monomer mixture for the first shell was added according to Table 1 at 7 mL/h. After 1 week of stirring, the addition of the monomer mixture for the second shell was performed dropwise (10 mL/min), and the dispersion was stirred overnight.

After end capping, the material was dissolved in THF, and the PDMS chains were removed by ultrafiltration. The complete removal was checked by GPC. After evaporation of the solvent, 0.3–0.5 g of clear, oily PDMS (45–75% with respect to 100% conversion of the alkoxy groups) and 1.2–1.5 g of white powder were obtained (sample code Sx-S; x indicates the amount of ClBz-T monomer [w/w]).

IR,  $\tilde{\nu}/\text{cm}^{-1}$ : 2963, 2907 (s)  $\nu(\text{CH}_3)$ ,  $\nu(\text{CH}_2)$ , 1606 (m)  $\nu$ -(aromatic ring), 1410 (s)  $\delta(\text{CH}_3)$ ,  $\delta(\text{CH}_2)$ , 1263 (vs)  $\delta_s(\text{SiCH}_3)$ , 1096, 1030 (vs)  $\delta_{\text{as}}(\text{Si}-\text{O}-\text{Si})$ , 847, 800 (s)  $\delta(\text{SiCH}_3)$ .

<sup>1</sup>H NMR,  $\delta/\text{ppm}$ : 0–1.5 (s, br,  $\text{SiCH}_3$ ), 4.5 (m, br,  $\text{CH}_2\text{Cl}$ ), 7.0–8.0 (s, br, aromatic H).

**Quaternization Reaction.** In a typical reaction, 1.0 g of nanospheres was dissolved in THF under argon atmosphere. According to the chloromethylphenyl content, a 1.1-fold molar excess of dimethylaminoethanol together with a small amount of cesium iodide were added. The reaction mixture was stirred for 2 weeks at room temperature. Finally, the THF was replaced by toluene by repeated rotary evaporation. Special care was taken to avoid drying of the sample. The degree of quaternization was analyzed by elemental analysis (sample code: Q precedes the sample code of the nonquaternized material; e.g., C4-S becomes QC4-S).

## Results and Discussion

A schematic overview of the synthesis of the poly-(organosiloxane) nanospheres is given in Figure 1. The first step of the synthesis is the sequential co-condensation of the different alkylalkoxysilane monomer mixtures in aqueous dispersion, followed by the end capping of reactive SiOH groups with ethoxytrimethylsilane (M). This allows the transfer into organic solvents. At this stage the reaction of the SiOH groups is not quantitative. The residual SiOH groups are again reacted with hexamethyldisilazane (HMN) in the organic phase which yields redispersable particles in solvents such as toluene, tetrahydrofuran or chloroform.

The synthesis of the core–shell spheres (Figure 1a) starts with the condensation of a mixture of trimethoxymethylsilane (T), (chloromethylphenyl)trimethoxysilane (ClBz-T), and diethoxydimethylsilane (D), which form the core. Subsequent addition of a mixture of D and T produces the hydrophobic shell.

The synthesis of core–shell–shell nanoparticles with PDMS core is performed in two different ways. The first consists of the condensation of pure D forming the core comprising linear PDMS chains, followed by the co-condensation of D/T/ClBz-T, resulting in the first shell. For the second hydrophobic shell, a mixture of D and T is added. Figure 1b shows schematically that the PDMS chains of the core are chemically linked to the surrounding network. This is avoided if the SiOH end groups of the linear PDMS chains are reacted with monofunctional units (M) before the monomers for the first shell are added. As shown in Figure 1c, the linear chains may be removed by ultrafiltration, leading to the formation of hollow (shell–shell) spheres. A subsequent quaternization of dimethylaminoethanol with the



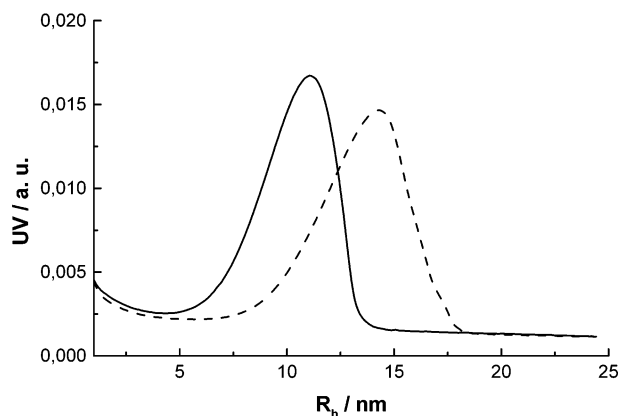


**Figure 2.** AF-FFF fractogram of the aqueous dispersion of C-S12-S after formation of first shell (line), and after formation of the outer shell (dashed).

chloromethylphenyl groups results in the formation of amphiphilic nanospheres (Figure 1d, preceding Q in the sample codes).

**Aqueous Dispersion.** The characterization of the nanospheres in the aqueous dispersion is particularly difficult due to the presence of free surfactant.<sup>13</sup> In each case, the dispersion is analyzed with asymmetric flow field-flow fractionation (AF-FFF) and dynamic light scattering (DLS) after formation of the functionalized core (C $x$ -S) or the functionalized first shell (C-S $x$ -S, S $x$ -S), and subsequently after formation of the nonfunctionalized shell.  $x$  indicates the amount of (chloromethylphenyl)trimethoxysilane (ClBz-T, w/w) employed in the synthesis. It was not possible to characterize the particle emulsion of the pure PDMS chains (core) (C-S $x$ -S, S $x$ -S) with AF-FFF, because the emulsion was not stable against shear induced by the flow. In Figure 2, the fractograms of C-S12-S obtained with AF-FFF are given.

Clearly, the increase in the radius upon addition of the inert shell is observed. As already shown for the nonfunctional nanospheres,<sup>13</sup> the amount of D present in the monomer mixture influences the number of growing particles. The size of the particles does not depend on the investigated ratios of ClBz-T/T at fixed total trifunctional monomer content. A separation of the relaxation modes observed in dynamic light scattering (DLS) was accomplished by employing a biexponential fit to the correlation function. The faster relaxation is attributed to the growing particles. This is especially important during the beginning of the synthesis, when a relatively high amount of free surfactant is present in the system and the particles are smaller than approximately 10 nm. The increase of the particle size is accompanied by an increase in the average relaxation times after addition of the second, nonfunctional shell. A major problem of the characterization with DLS arises from the difficulty to properly separate the two relaxation processes, which leads to substantially larger errors in the determination of the respective particle radii as compared to AF-FFF. The complete data for the AF-FFF and DLS analysis in the aqueous dispersion are given in Table 2.

For the reasons given above, the discussion of the shell thicknesses is based on the AF-FFF results, only. From the difference between the size of the core or core plus first shell, respectively, and the size of the particles after formation of the outer shell the thickness of the nonfunctionalized shell is determined. It varies between

**Table 2.** Hydrodynamic Radius  $R_h$  of the Nanospheres in Aqueous Dispersion, Obtained by AF-FFF and DLS, Respectively, and Second Cumulant  $\mu_2$ , Obtained at 90° Scattering Angle

sample		AF-FFF	DLS	
		$R_h$ /nm	$R_h$ /nm	$\mu_2$
C4-S	core	7.0	9.6	0.07
	shell	8.6	9.2	0.11
C8-S	core	6.7	8.7	0.05
	shell	8.8	9.8	0.08
C12-S	core	6.5	7.4	0.11
	shell	7.8	8.1	0.11
C-S4-S	1st shell	10.4	13.8	0.08
	2nd shell	13.7	14.2	0.04
C-S8-S	1st shell	10.4	14.0	0.08
	2nd shell	13.8	15.3	0.06
C-S12-S	1st shell	10.8	14.8	0.09
	2nd shell	13.6	14.7	0.04
S4-S	1st shell	12.7	14.3	0.04
	2nd shell	15.1	16.0	0.04
S8-S	1st shell	12.2	14.2	0.04
	2nd shell	15.4	15.6	0.03
S12-S	1st shell	12.1	13.9	0.04
	2nd shell	15.2	15.4	0.02

1.5 and 3 nm and corresponds well to the amount of added monomer. Due to the already discussed influence of the free surfactant, DLS yields slightly higher values. It should be mentioned that AF-FFF does not yield the mass distribution of the radii, because with the applied UV detection only the surfactant covering the surface and the ClBz-T units are detected. This also makes a quantitative comparison to the  $\langle 1/R_h \rangle^{-1}_z$  average radius obtained by DLS extremely complicated which is beyond the scope of the present paper.

**Redispersable Nanospheres.** The nanospheres in the aqueous dispersion still bear reactive SiOH groups on the particle surface, which lead to an irreversible aggregation if the particles are precipitated at this point of the synthesis and have to be at least partly saturated. To avoid interparticle condensation, the monofunctional silane M is added, which also destabilizes the particles in aqueous dispersion. Subsequently, the wet particles are transferred into toluene, where the residual SiOH groups are reacted with hexamethyldisilazane (HMN) quantitatively. The success of this procedure crucially depends on the water content of the particles to be dispersed in toluene. If the particles are too dry, interparticle condensation may have occurred, whereas too wet particles are not quantitatively end capped. Thus, a small amount of aggregated particles may result. Afterward, the poly(organosiloxane) nanoparticles are precipitated and dried. All samples are redispersable in organic solvents such as toluene or tetrahydrofuran. The average sizes of the particles as determined by DLS are given in Table 3.

In addition to the cumulant fit, the data were also analyzed by a biexponential fit, and the fast relaxation was attributed to the poly(organosiloxane) nanoparticles and the second, slower relaxation to partly aggregated particles. The appearance of aggregates (see above) and thus the increase in the polydispersity increases the problem of size determination with DLS. Nevertheless, the particle sizes obtained in the aqueous dispersion and in toluene, respectively, are in reasonable good agreement.

In the case of samples S $x$ -S, the PDMS chains, which have molecular weights of 1000–3000 g/mol,<sup>10</sup> were removed by ultrafiltration, which was monitored by GPC as shown for S12-S in Figure 3a.

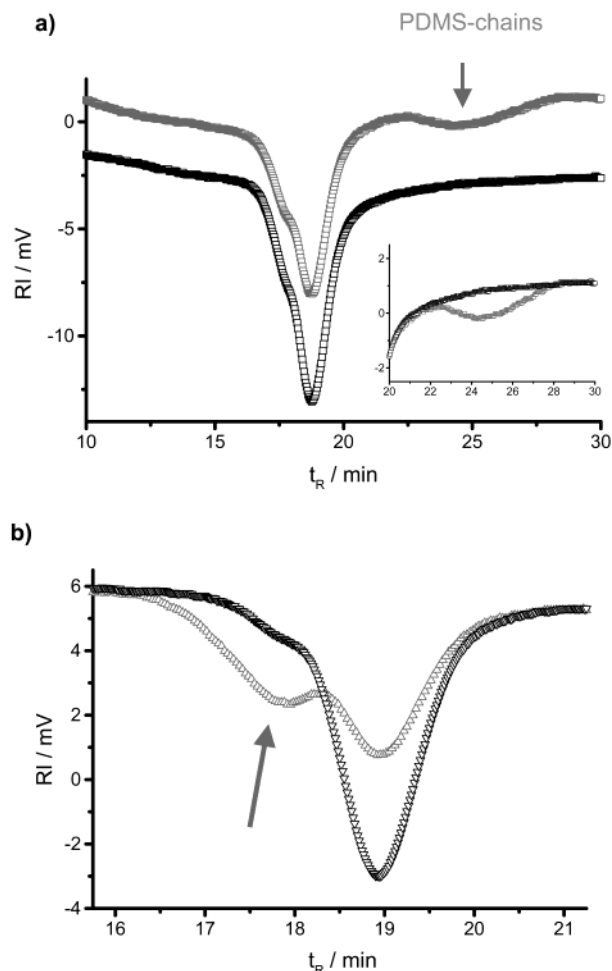


**Figure 3.** (a) GPC chromatogram of S8-S in toluene before (gray) and after ultrafiltration (black). The insert shows the removal of the PDMS. (b) Aging of sample S12-S observed with GPC in toluene, when the sample is stored as powder. Key: black, after synthesis; gray, 4 weeks later. The arrow indicates the increasing amount of aggregates.

**Table 3. Hydrodynamic Radius  $R_h$  and Second Cumulant  $\mu_2$  (90°), Obtained by DLS, for the Nanospheres in Aqueous Dispersion, in Toluene and after Quaternization in Toluene (Concentration  $c = 1$  g/L)**

sample	water		toluene		toluene	
	$R_h$ /nm	$\mu_2$	$R_h$ /nm	$\mu_2$	sample	$R_h$ /nm $\mu_2$
C4-S	9.2	0.11	10.5	0.05	QC4-S	10.2 0.06
C8-S	9.8	0.08	11.1	0.09	QC8-S	11.0 0.10
C12-S	8.1	0.11	9.6	0.07	QC12-S	8.3 0.24
C-S4-S	14.2	0.04	14.8	0.06	QC-S4-S	15.6 0.06
C-S8-S	15.3	0.06	16.6	0.12	QC-S8-S	16.7 0.04
C-S12-S	14.7	0.04	15.1	0.13	QC-S12-S	16.5 0.14
S4-S	16.0	0.04	16.5	0.05	QS4-S	17.5 0.02
S8-S	15.6	0.03	17.4	0.08	QS8-S	18.1 0.08
S12-S	15.4	0.02	16.5	0.13	QS12-S	16.9 0.14

This separation is possible, because the network density or microporosity of the shell is large enough and can be controlled by the ratio of D/T.<sup>10</sup>

It has already been shown that the poly(organosiloxane) nanoparticles carrying chloromethylphenyl functionalities tend to age within several weeks to months if stored in powder form.<sup>14,15</sup> The end capping seems to be influenced by the presence of the functional groups. The thickness of the nonfunctionalized shell is determined to vary between 1.5 and 3 nm as analyzed in the aqueous dispersion. This thickness seems to be necessary to prevent the interparticle condensation, which

**Table 4. Amount of (Chloromethylphenyl)siloxane in the Nanospheres, Determined by UV/Vis Spectroscopy (exptl), Compared to the Calculated (calcd) Values (at 100% conversion with Respect to the Monomers and Neglecting the Surface Modification) and Amount of ClBz-T, Which Participated in the Quaternization Reaction, Determined by Elemental Analysis (quatern)**

sample	amt of ClBz-T (w/w), calcd	amt of ClBz-T (w/w), exptl	sample	amt of ClBz-T (w/w), quatern	deg of quaternization (%)
C4-S	5.7	5.8	QC4-S	1.3	22.4
C8-S	11.2	7.9	QC8-S	2.0	25.3
C12-S	16.6	14.3	QC12-S	8.2	57.3
C-S4-S	5.7	6.3	QC-S4-S	2.0	31.7
C-S8-S	11.2	10.5	QC-S8-S	3.5	33.3
C-S12-S	16.6	16.5	QC-S12-S	11.1	67.3
S4-S	8.3	6.7	QS4-S	4.0	59.7
S8-S	16.2	16.4	QS8-S	8.9	54.3
S12-S	23.8	20.0	QS12-S	11.5	57.5

is known to take place with pure ClBz-T particles. However, for the encapsulation of hydrophilic small molecules the mesh size of the shell-forming network as well as the shell thickness represent important parameters. For fast penetration of small molecules through the surface network the shell should be as thin as possible. However, for thin shells, aging of the samples, i.e., particle aggregation, becomes more pronounced but could be minimized by storing the samples in solution. Unfortunately, the mesh size of the surface network cannot be increased beyond 30% D content because this leads to an unstable dispersion.<sup>10,16</sup> The effect of the aging is analyzed with GPC in toluene, and the results are shown in Figure 3b for sample S12-S after the synthesis and 4 weeks later. The main peak at higher retention times corresponds to the poly-(organosiloxane) nanoparticles; the earlier peak is attributed to aggregates. The aging of some of the samples between the synthesis and characterization is also reflected in an increased second cumulant  $\mu_2$  (see Table 3).

The relative content of ClBz-T (w/w) in the poly-(organosiloxane) nanoparticles was determined by UV spectroscopy at  $\lambda = 224$  nm, and compared to the theoretical values (Table 4). The amount of ClBz-T incorporated into the particles corresponds well to the monomer feed, as expected.

Atomic force microscopy is employed to visualize the particles. Figure 4 displays AFM images (tapping mode) of C4-S, C-S4-S, and S4-S, respectively.

The radii of the particles were determined to be  $8.5 \pm 0.5$  nm for C4-S,  $12.3 \pm 2.1$  nm for C-S4-S, and  $15.3 \pm 2.1$  nm for S4-S, comparable to the radii found by DLS. Similar results are obtained for the other samples. The height of the particles is also characterized by AFM. For sample C4-S, the average height is determined to be 14.2 nm, which corresponds to 84% of the diameter and reflects the elastic properties of the D/T network. This internal network structure is found to relax even more for C-S4-S, which has a PDMS core. In this case, the average height is determined to be 17.4 nm, which relates to 71% of the diameter. For S4-S, where the PDMS chains were removed from the core, the average height is found to be 14.7 nm, which is only 48% of the diameter. This value corresponds very nicely to the height of a deflated hollow sphere. The hollow core radius may be estimated, based on the AF-FFF measurements and the different volume fractions of the added monomer mixtures, to be 7.5 nm. The typical

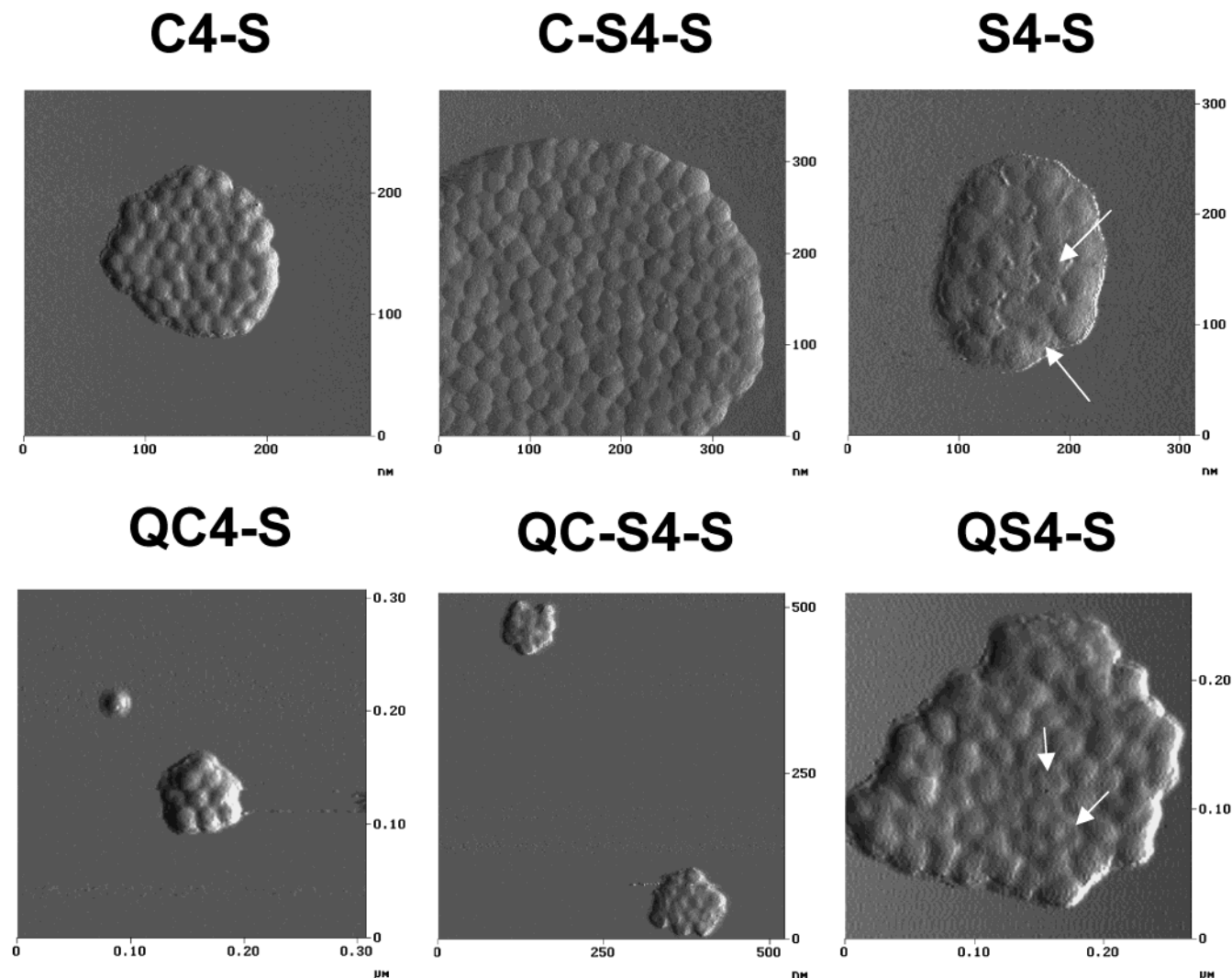


**Figure 4.** AFM (tapping mode, amplitude) of the samples C4-S, C-S4-S, S4-S, QC4-S, QC-S4-S, and QS4-S, spin cast from toluene onto mica. Arrows indicate the deflated hollow sphere structure.

surface pattern of deflated hollow spheres is also observed in the AFM images and indicated by the arrows in Figure 4. Currently we are working on the visualization of the hollow sphere structure of samples Sx-S by imaging with Cryo-TEM, which is very difficult due to the cross-linked nature of the shell and the necessity to use organic solvents. Nevertheless, SAXS measurements and AFM investigations of nonfunctionalized nanoparticles strongly indicate the hollow sphere structure.<sup>10</sup>

**Formation of Amphiphilic Nanospheres by Quaternization.** The quaternization of dimethylaminoethanol with chloromethylphenyl groups results in the formation of ionic moieties (Figure 1d). The amount of ClBz-T groups, which participated in the quaternization reaction, was determined by elemental analysis and the results are given in Table 4. The ratio of the amount of quaternized ClBz-T to the experimentally determined content of ClBz-T yields the degree of quaternization. Under identical conditions the degree of quaternization seems to increase with increasing mass fraction of ClBz-T, the origin of which is unknown and might even be accidental. However, by increasing the mass fraction of ClBz-T in the core or shell, respectively, it is possible to control the local hydrophilic properties within the nanoparticles. In the future, this is going to be used to

correlate the uptake of small hydrophilic molecules, such as dyes, into the nanospheres with the amount of ionic groups present in the network.

Figure 4 shows the AFM images obtained from the quaternized samples, spin cast from toluene. The radii of the particles are determined to  $9.9 \pm 0.7$  nm for QC4-S,  $12.1 \pm 1.2$  nm for QC-S4-S and  $15.5 \pm 2.2$  nm for QS4-S, respectively, corresponding well to the hydrodynamic radii observed by DLS (Table 3) and also to the values obtained before quaternization. Again, the determination of the exact internal structure of the hollow particles by DLS in solution is difficult due to the influence of the polydispersity. For nonfunctionalized poly(organosiloxane) nanospheres, the hollow sphere structure was shown by Emmerich et al.<sup>10</sup> with a sample of very low polydispersity by small-angle X-ray scattering experiments. Cryo-TEM experiments are planned in order to corroborate the hollow sphere structure.

Currently, these nanospheres are investigated as containers for the encapsulation of hydrophilic probes such as water-soluble dyes, and as nanoreactors for the synthesis of metal colloids inside the spheres.<sup>17</sup>

## Conclusion

The synthesis of new amphiphilic core-shell poly(organosiloxane) nanospheres was successfully per-

formed. The obtained model particles are well suited to study the sequestration and encapsulation of small hydrophilic molecules in organic solvents. The different degrees of functionalization make it possible to investigate quantitatively, whether the uptake is related to the amount of hydrophilic groups within the nanoparticles.

**Acknowledgment.** We would like to thank Norbert Hugenberg for the AFM measurements, the Wacker Chemie for monomers and financial support, and the BMBF (FKZ 03C0288A8) and the Fonds der Chemischen Industrie for financial support.

## References and Notes

- (1) (a) Zhou, J. Y.; Li, Z.; Liu, G. J. *Macromolecules* **2002**, *35*, 3690. (b) Stewart, S.; Liu, G. J. *Chem. Mater.* **1999**, *11*, 1048. (c) Ding, J. F.; Liu, G. J. *J. Phys. Chem. B* **1998**, *102*, 6107. (d) Ding, J. F.; Liu, G. J. *Macromolecules* **1998**, *31*, 6554. (e) Henselwood, F.; Liu, G. J. *Macromolecules* **1998**, *31*, 4213.
- (2) (a) Kao, H. M.; O'Connor, R. D.; Mehta, A. K.; Huang, H. Y.; Poliks, B.; Wooley, K. L.; Schaefer, J. *Macromolecules* **2001**, *34*, 544. (b) Zhang, Q.; Remsen, E. E.; Wooley, K. L. *J. Am. Chem. Soc.* **2000**, *122*, 3642. (c) Huang, H. Y.; Remsen, E. E.; Kowalewski, T.; Wooley, K. L. *J. Am. Chem. Soc.* **1999**, *121*, 3805. (d) Thurmond, K. B.; Kowalewski, T.; Wooley, K. L. *J. Am. Chem. Soc.* **1997**, *119*, 6656.
- (3) (a) Maskos, M.; Harris, J. R. *Macromol. Rapid Commun.* **2001**, *22*, 271. (b) Rheingans, O.; Hugenberg, N.; Harris, J. R.; Fischer, K.; Maskos, M. *Macromolecules* **2000**, *33*, 4780.
- (4) (a) Shi, X. Y.; Caruso, F. *Langmuir* **2001**, *17*, 2036. (b) Tiourina, O. P.; Antipov, A. A.; Sukhorukov, G. B.; Larinova, N. L.; Möhwald, H. *Macromol. Biosci.* **2001**, *1*, 209. (c) Park, M. K.; Xia, C. J.; Advincula, R. C.; Schutz, P.; Caruso, F. *Langmuir* **2001**, *17*, 7670. (d) Caruso, F.; Trau, D.; Möhwald, H.; Renneberg, R. *Langmuir* **2000**, *16*, 1485. (e) Caruso, F.; Caruso, R. A.; Möhwald, H. *Chem. Mater.* **1999**, *11*, 3309. (f) Donath, E.; Sukhorukov, G. B.; Caruso, F.; Davis, S. A.; Möhwald, H. *Angew. Chem., Int. Ed.* **1998**, *37*, 2202.
- (5) Baumann, F.; Schmidt, M.; Deubzer, B.; Geck, M.; Dauth, J. *Macromolecules* **1994**, *27*, 6102.
- (6) Baumann, F.; Deubzer, B.; Geck, M.; Dauth, J.; Schmidt, M. *Macromolecules* **1997**, *30*, 7568.
- (7) Baumann, F.; Deubzer, B.; Geck, M.; Dauth, J.; Sheiko, S.; Schmidt, M. *Adv. Mater.* **1997**, *12*, 955.
- (8) Stöber, W.; Fink, A.; Bohn, E. *J. Colloid Interface Sci.* **1968**, *26*, 62.
- (9) (a) van Blaaderen, A.; Vrij, A. *J. Colloid Interface Sci.* **1993**, *156*, 1. (b) van Blaaderen, A.; Vrij, A. In *The Colloid Chemistry of Silica*; Bergna, H. E. Ed.; Advances in Chemistry Series 234, American Chemical Society: Washington, DC, 1994.
- (10) Emmerich, O.; Hugenberg, N.; Schmidt, M.; Sheiko, S.; Baumann, F.; Deubzer, B.; Weis, J.; Ebenhoch, J. *Adv. Mater.* **1999**, *11*, 1299.
- (11) Berne, B. J.; Pecora, R. *Dynamic Light Scattering*; J. Wiley, New York, 1976.
- (12) Tank, C.; Antonietti, M. *Macromol. Chem. Phys.* **1996**, *197*, 2943.
- (13) Jungmann, N.; Schmidt, M.; Maskos, M. *Macromolecules* **2001**, *34*, 8347.
- (14) Graf, C.; Ph.D. Thesis, University of Mainz, Germany, 1999.
- (15) Jungmann, N.; Ph.D. Thesis, University of Mainz, Germany, 2000 (<http://archimed.uni-mainz.de/>).
- (16) Roos, C.; Schmidt, M.; Ebenhoch, J.; Baumann, F.; Deubzer, B.; Weis, J. *Adv. Mater.* **1999**, *11*, 761.
- (17) Maskos, M.; Jungmann, N.; Schmidt, M. *Polym. Prepr.* **2001**, *42*, 90.

MA012145B